

## Loose Gangues Backfill Body's Acoustic Emissions Rules During Compaction Test: Based on Solid Backfill Mining

Junmeng Li<sup>1</sup>, Yanli Huang<sup>1,\*</sup>, Wenyue Qi<sup>1</sup>, Guoqiang Kong<sup>1</sup> and Tianqi Song<sup>1</sup>

**Abstract:** In fully mechanized solid backfilling mining (FMSBM), the loose gangues backfill body (LGBB) that filled into the goaf becomes the main body of bearing the overburden load. The deformation resistance of LGBB is critical for controlling overburden movement and surface subsidence. During the process of load bearing, LGBB will experience grain crushing, which has a significant effect on its deformation resistance. Gangues block will be accompanied with obvious acoustic emissions (AE) features in process of slipping, flipping and damaging. Under confined compression test, monitoring the AE parameters of LGBB can reveal the impact mechanism of grain crushing on LGBB deformation. The study is of great significance for obtaining an in-depth understanding of the mechanical properties of LGBB, and providing guidance to the engineering practice of FMSBM. In order to study the rules of acoustic emissions (AE) of graded Loose gangues backfill body (LGBB) in confined compression test, this article introduces the AE systems to conventional confined compression test to monitor AE signals resulted from the friction and fragmentation among LGBB. The test results show that in the process of LGBB compaction, AE parameters are highly correlated with the strain-stress curve. AE events of balanced-sized graded gangues are more inactive than other two graded samples in different compression stages, AE events of large-particle-dominated graded gangues are most active. In the spatial distribution, AE events are the most active on the edges and the middle part of test samples and the phenomenon of grain crushing is the most obvious in these positions.

**Keywords:** Loose gangues backfill body, Confined compression, acoustic emission, space-time evolution, failure mechanism.

### 1 Introduction

LGBB is a discontinuous medium in nature and cohesionless, easily crushed bulk material. Along with the rapid development of solid backfill mining technology, it has become the main filling material in the goaf as the main body to assume the overburden load and mitigate surface subsidence [Miao, Zhang and Guo (2010); Miao (2012); Huang (2012)]. The deformation-resistant ability of LGBB is critical to the filling quality. Studies [Huang, Zhang, Zhang et al. (2012); Liu (2014); Wu (2014)] show that the movement and

---

<sup>1</sup>State Key Laboratory of Coal Resources and Safe Mining, School of Mines, China University of Mining & Technology, Xuzhou 221116, China

\* Corresponding author: Yanli Huang. Email: huangyanli6567@163.com

fragmentation during compression are the main contributing factor to the deformation of LGBB. Therefore, it is crucial to study the movement and fragmentation characteristics during compression to reveal the deformation mechanism. Currently, it mainly use alternative materials to study the characteristics of the movement and the failure of bulk material under the action of external forces. Particle material model tests are mainly achieved through the organic glass rods, metal rods, photoelastic materials etc. Zhong et al. [Zhong and Yuan (1992); Calvetti, Combe and Lanie (1997); Zhang, Zhang, Zhang et al. (2008)]. The advantage of this method is that the internal structure change of the simulated material during the deformation process can be observed easily and intuitively; In the microscopic test of actual material, CT (computerized tomography, abbreviated CT) technology is currently feasible, but used less in the test of the crushed gangue [Masad, Saadeh, Al-Rousan et al. (2005)]. The current CT test can only monitor two-dimensional space, there is a certain deviation between the monitoring information and the actual particle movement and fragmentation. So it still exists some disadvantages.

The acoustic emission feature parameters contain abundant omen information of damage progressive fracture [Lei, Masuda, Nishizawa et al. (2004)]. Currently, studies on the damage mechanism of blocks like coal-rock masses, concretes and cementing materials by acoustic emissions (AE) techniques are abundant and have achieved plenty of valuable results. For example, Mansurov [Mansurov (1994); Browning, Meredith, Stuart et al. (2017); Ingraham, Issen and Holcomb (2013); Michlmayr and Or (2012); Rudajev, Vilhelm and Lokajicek (2000)] monitored the AE information and predict the type of rock fragmentation that occurred. Li et al. [Li, Yue, Yang et al. (2016); Ai, Zhang, Liu et al. (2012)] through triaxial compression AE tests on coal-rock samples, analyzed the damage evolution features of limestone and studied the sequence, energy release and spatial evolution rules of AE in the fracture process of coal-rock. Meng et al. [Meng, Zhang, Han et al. (2016); Du, Li, Li et al. (2015)] conducted many tests on the entire process of rock failure under uniaxial compression and fatigue loading process, both utilizing AE techniques, and analyzed the mechanical properties and AE features in the process.

Comprehensive research situation at home and abroad, the current research of the mechanical properties of LGBB material are mainly concentrated in the macroscopic deformation characteristics, and lack of the mechanism of the influence of particle breakage on macroscopic deformation. At present, the application of AE technology in geotechnical engineering is mainly focused on the damage characteristics of intact rock mass, but less applied to bulk materials. Under the external compression, gangues block will be accompanied with obvious AE features in process of slipping, flipping and damage [Cao, Du, Li et al. (2017); Li, Zhang, Zhou et al. (2017); Lu, Song, Jia et al. (2015)]. In different loading stages, the movement and broken degree of particles within LGBB are different, which lead to different AE signals within various activity. Therefore, AE parameters of the LGBB materials under different compression stages were monitored and analyzed in this paper. It was aimed to study the particle breakage characteristics of LGBB in different compaction stages and to establish the relationship between AE parameters and particle breakage of LGBB.

## 2 Experiment design and material selection

### 2.1 The basic principle and three-dimensional location principle of AE

#### (1) The basic principles of AE

AE refers to the phenomenon that the material or structure releases its strain energy in the form of elastic waves in the process of deformation or destruction under loading [Qin, Li, Zhang et al. (1993)]. AE is a common physical phenomenon, most materials produce AE signals during deformation and fracture, but many of the AE signals strength is very weak, the human's ear can not hear directly, need a sensitive electronic instruments to detect. The monitoring and analysis of AE signals and the use of AE signals to infer the internal properties changes of materials and structures are called AE technologies. The AE detection principle is shown in Fig. 1. The elastic wave emitted from the AE source finally propagates to the surface of the material, causing the surface displacement that can be detected by the AE sensors. AE sensor converts mechanical vibrations of the material into electrical signals, which are then amplified, processed and recorded. Then the AE signals are analyzed and inferred to understand the mechanism of AE from the material.

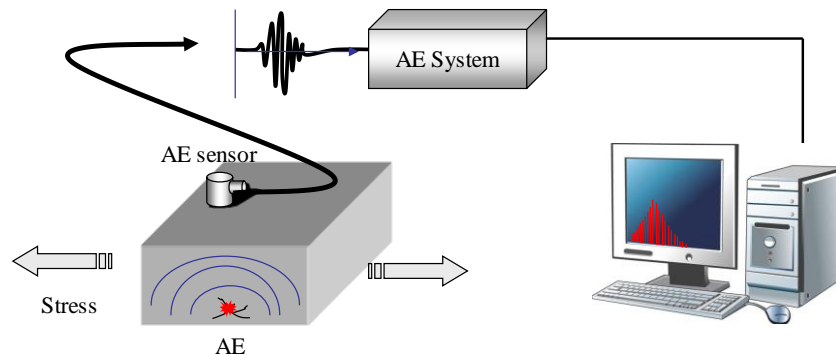


**Figure 1:** AE detection principle

LGBB under the external compression, gangues block will be accompanied with obvious AE features in process of slipping, flipping and damage. In different loading stages, the movement and broken degree of particles within LGBB are different, which lead to different AE signal within various activity, so we can study the particle breakage characteristics of LGBB in different stages of compaction by analyzing the AE signal activity level.

#### (2) Three-dimensional location principle of AE

The location of AE events is the first step to study the AE activity and microcrack growth of rock. The earliest AE three-dimensional location study is carried out by Scholz. He used a set of AE probes to form a probe array to determine the spatial position of each AE event in 1968. Now, the main location methods of AE event are Geiger location method, Bayesian method, Fedorov generalized least square method, relative location technology and simplex method [Geiger (1912); Tarantola and Valette (1982); Fedorvo (1974)]. The method of AE apparatus used in this paper is Geiger location method.

Three-dimensional location principle of AE events is to pick up arrival time difference of

the P-wave by different position sensors to invert the position of the AE event. Firstly, the arrival time of P-wave is identified, the simplex algorithm is used to invert the position of the AE event through time difference. The mathematical calculation principle (in P-wave picking example) is that assume the spatial coordinate of the AE event is  $(x, y, z)$ , the coordinate of the sensor is  $(x_i, y_i, z_i)$ , velocity of P-wave to  $V_p$ , The time point at which an AE event occurs is  $t$ , the time point at which the AE signal is transmitted to the sensor  $i$  is  $t_i$ , the distance from the AE source to the sensor  $i$  has the following relationship:

$$\sqrt{(x-x_i)^2 + (y-y_i)^2 + (z-z_i)^2} = v_p(t_i - t) \quad (1)$$

At least three sensors are arranged to obtain the following equations:

$$\begin{cases} \sqrt{(x-x_1)^2 + (y-y_1)^2 + (z-z_1)^2} = v_p(t_1 - t) \\ \sqrt{(x-x_2)^2 + (y-y_2)^2 + (z-z_2)^2} = v_p(t_2 - t) \\ \sqrt{(x-x_3)^2 + (y-y_3)^2 + (z-z_3)^2} = v_p(t_3 - t) \end{cases} \quad (2)$$

The coordinates  $(x, y, z)$  of the AE source can be obtained by solving the Eq. (2), and the three-dimensional location of the AE event can be achieved.

## 2.2 Experiment design

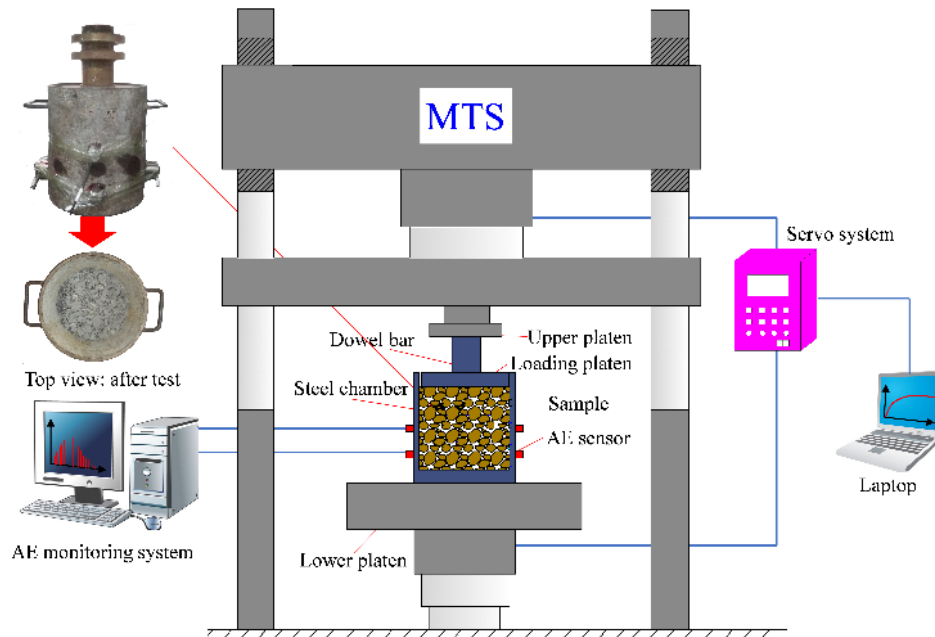


**Figure 2:** Experiment system and installation of AE sensors

The loading control systems (MTS815.02 electro-hydraulic servo testing machine of rock mechanics) and AE monitoring systems (PCI-2 model produced by Physical Acoustic Corporation) are employed in the experiment. The PCI-2 systems can count AE events and store AE parameters automatically, communicate with computers and manage to monitor and locate AE events in real time, the AE monitoring systems is shown in Fig. 2. A circular steel cylinder (height: 270 mm, inner diameter: 250 mm, loading height: 230 mm) is installed to contain LGBB samples. Six Nano30 AE sensors (The sensor has the best working frequency, the operating frequency of the Nano30 AE sensor is 100 kHz~400 kHz. So select the high pass filter for 100 kHz, low-pass filter for 400 kHz.) are evenly placed on the upper and lower bound of the cylinder. To ensure the coupling effect, albany grease is spread on the contact area between the sensors and the cylinder ektexine, air is squeezed out and tape is employed to ensure that the sensors are firmly stuck on the steel cylinder, the layout diagram of sensors is shown in Fig. 3.

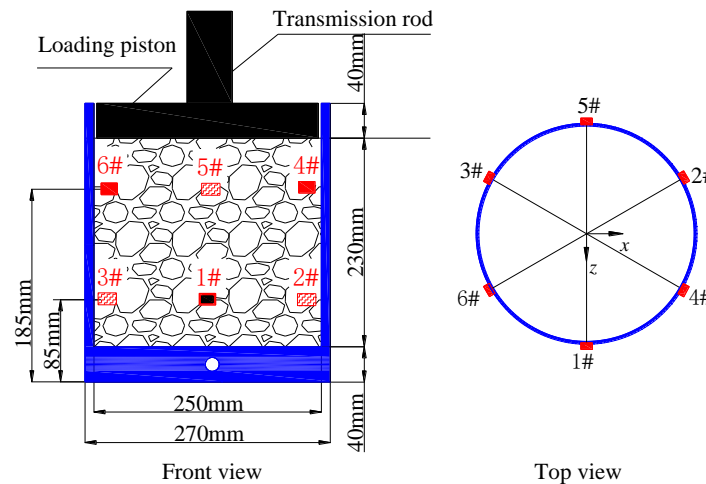


**Figure 3:** Layout diagram of sensors

The sampling frequency of the six channels of the AE system is set at 5 MSPS (5 MHz). The gain of preamplifier is 40 dB. The high pass filter and low pass filter of the analog filter are 100 kHz and 400 kHz respectively. Considering that AE signals are sensitive to surrounding noises, we often adopt threshold setting method to reduce noise [Mao, Aoyama, Goto et al. (2015)]. In the early stage of the experiment, we made the load control system run for a while and monitored the acoustic emission simultaneously. According to continuous adjusting of the threshold, we found that when the fixed threshold is set at 45 dB, the noises can be largely blocked out. Finally the fixed threshold is set at 45 dB.

When the experiment running, the loading systems and AE monitoring systems are synchronized. The axial strain control loading method is employed in the loading system, with the loading rate being 5.0 mm/min. The loading will stop when axial stress hits 21 MPa. During the loading process, the system automatically collects and records the load, deformation and other parameters. For the application of AE monitoring technology in the field of coal and rock, the AE parameters change with time were to evaluate the coal and

rock damage degree. In the field of geotechnical engineering, the AE parameters such as ring-down counts ( $N$ ), the cumulative of ring-down counts ( $\Sigma N$ ), and AE events are commonly used to analyze the AE characteristics of damage rupture of coal rock mass under external load [Mansurov (1994); Calvetti, Combe and Lanie (1997); Ai, Zhang, Liu et al. (2012); Ingraham, Issen and Holcomb (2013); Browning(2017)].

Ring-down counts ( $N$ ): The oscillation frequency of AE signals over threshold is used to evaluate AE activity.

Cumulative of ring-down counts  $\Sigma N$ : Displays the total ring-down counts recorded before the analyzed time point.

AE events: The same AE hit is detected by multiple channels simultaneously and can be used for AE positioning.

### **2.3 Material selection**

The material can be categorized into four types, according to the mineralogy characteristics of gangue [Wang (2005)]: clay mineral, sandstone, carbonate rock, and alumina mineral. The gangue used in solid filling coal mining mainly comes from two sources. One source is the rock material that produced during the excavation process of rock roadway and coal roadway; the gangue from this source is called “excavation gangue,” which mainly consists of sandstone. The other source is the rock material that discharged from the coal washing process. The gangue from this source is called “washing gangue.” The experimental study takes solid filling coal mining face in Tangkou Coal Mine as the project background. The goaf is filled with gangues from its gangue dump, which lithology is sandstone. Therefore, the gangue is a representative study subject for the research. Gangue blocks is the angular convex polyhedron structure with different shape and size, the main chemical composition is  $\text{SiO}_2$ ,  $\text{Al}_2\text{O}_3$  etc, Containing alkali, alkaline earth metal, sulfide, organic matter etc, the density is  $2.12 \times 10^3 \text{ kg} \cdot \text{m}^{-3}$ . To study the AE features of different graded gangues in different compression stages, three types of gangues, i.e. balanced-sized, large-particle-dominated and small-particle-dominated graded gangues, are prepared with a grading sieve. Gradation details of three test samples are demonstrated in Tab. 1 and gangue samples of different particle sizes in Fig. 4(a-e).

**Table 1:** Gradation Plan of LGBB Test samples

Gradation	Volume Percentage of Different-Sized Blocks /%				
	20-30 mm	30-40 mm	40-50 mm	50-60 mm	60-70 mm
#1	20	20	20	20	20
#2	-	-	-	30	70
#3	70	30	-	-	-

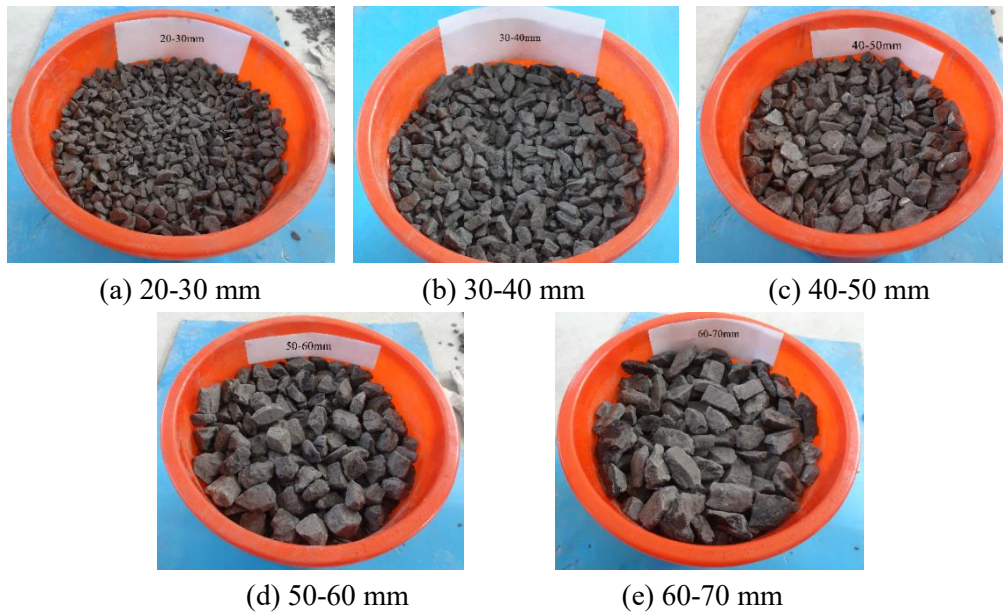


**Figure 4:** Test samples of LGBB of different particle sizes

**2.4 Basic properties test of the material**

(1) Mineral composition test of experiment material

The mineral composition test results of sandstone type “excavation gangue” used in this experiment are shown in Fig. 5 and Tab. 2.

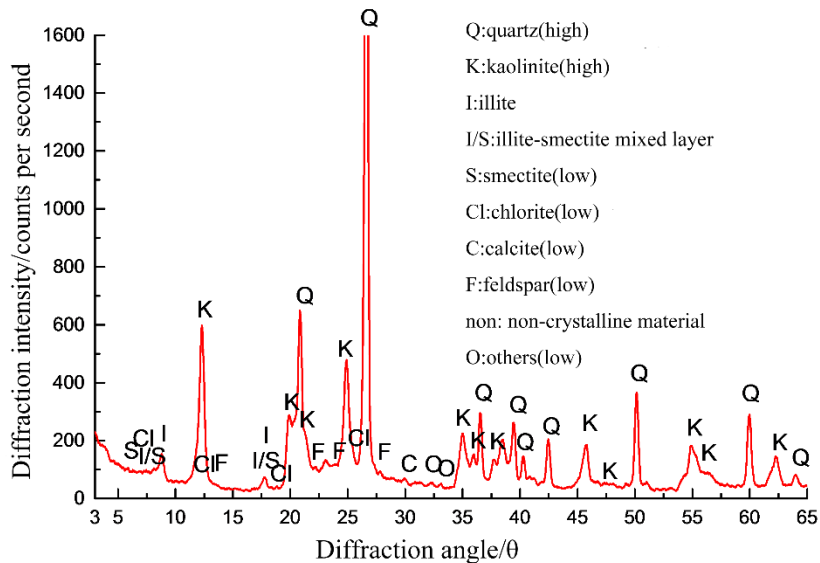


**Figure 5:** XRD analysis

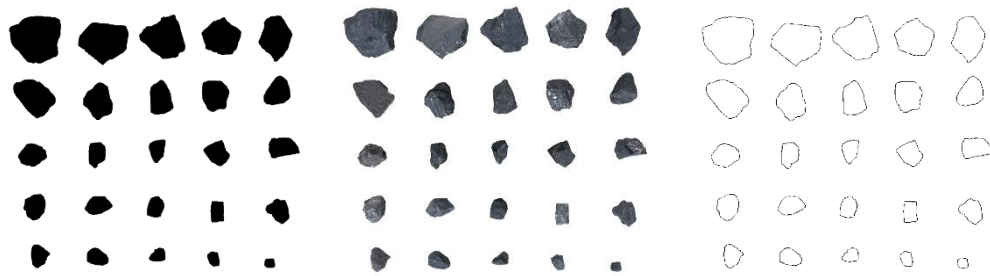
**Table2:** Mineral composition and chemical composition (%)

Mineral composition	Quartz	Kaolinite	Illite	Illite-smectite mixed layer	Smectite
Content (%)	37	35	12	6	1
Mineral composition	Chlorite	Feldspar	Calcite	Non-crystalline material	Others
Content (%)	2	1	0.5	4	1.5
Chemical composition	Na <sub>2</sub> O	MgO	Al <sub>2</sub> O <sub>3</sub>	SiO <sub>2</sub>	K <sub>2</sub> O
Content (%)	1.2	1.2	24.3	53.1	1.3
Chemical composition	CaO	Fe <sub>2</sub> O <sub>3</sub>	P	S	others
Content (%)	5.4	1.9	0.003	0.8	10.77

According to the test results, it can be obtained that the sandstone type “excavation gangue” is mainly composed of two kinds of minerals, quartz and kaolinite accounting for 72% of the total, of which quartz occupies the largest proportion of 37%, the sandstone type “excavation gangue” also has some illite, illite-smectite mixed layer and a small amount of chlorite, smectite, feldspar and other minerals. The chemical composition of sandstone type “excavation gangue” mainly consists of SiO<sub>2</sub> and Al<sub>2</sub>O<sub>3</sub>, accounting for 77.4% of the total, of which SiO<sub>2</sub> occupy the largest proportion, reaching 53.1%. Therefore, sandstone type “excavation gangue” has high hardness and deformation resistance.

## (2) Statistical analysis of shape of the gangue block

The filling gangue used in the fully mechanized solid backfilling coal mining are those treated by crushing and sieving, and the particle size is usually 0 mm~70 mm. In this paper, ImageJ image processing software is used to carry out statistical analysis of the shape of gangue of different diameters used in solid filling mining. The detailed analysis procedures are as follows: ① Use digital camera to capture high-definition digital images of randomly selected gangue blocks (shown in Fig. 6(a)); ② Two value processing is performed on the imported digital image, using the ImageJ image processing software. (shown in Fig. 6(b)); ③ The boundary contour of the gangue block is extracted using the Analyze particles function of ImageJ image processing software (shown in Fig. 6 (c)).



(a) High-definition digital image (b) Two value image (c) The boundary contour image

**Figure 6:** Statistical analysis of shape of the gangue block

According to statistical analysis, the gangue particles are generally irregular convex polyhedron in shape and the length of long axis and short axis is approximation.

### 3 Features of deformation-resistance and failure of graded gangues during confined compression

#### 3.1 Strain-stress ( $\varepsilon$ - $\sigma$ ) curve of LGBB during confined compression

The macroscopic deformation characteristics of LGBB are the key factors to control overburden movement and determine the filling quality, while the LGBB can be crushed in the loading process, which has a significant impact on its macroscopic deformation-resistant ability. In order to reveal the influencing mechanism of particle crushing to LGBB macroscopic deformation, it is necessary to establish the relationship between the macroscopic deformation and granular crushing of LGBB, and obtaining the stress-strain relation (Fig. 7) of LGBB in the compression process is the basis.

Three grades of LGBB (five groups for each grade, 15 groups in total) are prepared for the confined compression test. Three complete confined compression tests are conducted to each one of the three graded LGBB. The average of the 3 tests was taken as the final test result. The resulted strain-stress ( $\varepsilon$ - $\sigma$ ) curves are shown in Fig. 7. In this paper, the macroscopic stress-strain relation of LGBB is divided into some stages according to the change rate of the stress along with the strain during the compression process of LGBB. By taking the first derivative of each curve of Fig. 7, the change rate of the stress along with the strain during the compression process of LGBB was obtained, as shown in Fig. 8. In this paper, when the stress rate is not more than 20 MPa, change rate is very slow, which means the stress increases with the strain almost uniformly, the stress-strain curve at this stage is divided into the approximate linear stage; When the stress rate is between 20 MPa and 85 MPa, change rate is quite fast, the stress increases exponentially with the strain, the stress-strain curve at this stage is divided into the slope fast increase stage; when the stress rate is beyond 85 MPa, the stress - strain curve at this stage is divided into the stable linear stage.

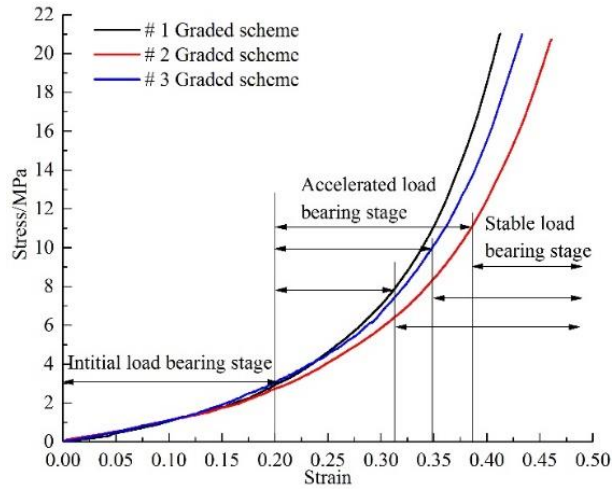


**Figure 7:**  $\sigma$ - $\varepsilon$  Curves of graded LGBB during confined compression

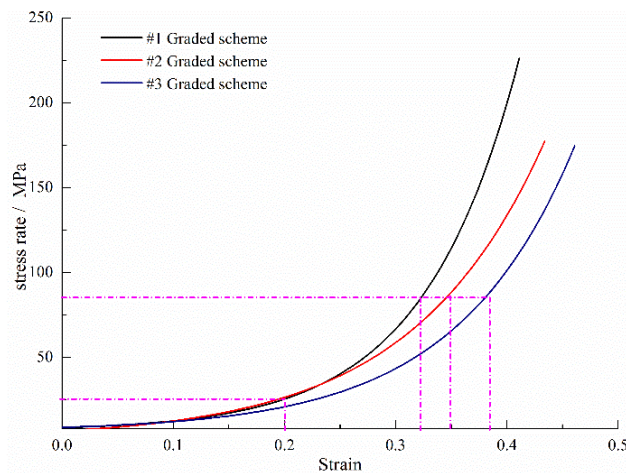


**Figure 8:** Stress rate-strain curve of different graded LGBB

Fig. 7 and Fig. 8 demonstrate that:

(1) As the load stress going up, the stress is divided by the change rate of strain, the deformation process of graded LGBB can be divided into three stages: the approximate linear stage, the slope fast increase stage and the stable linear stage. In the approximate linear stage, LGBB' deformation-resistant ability is still low, and they tend to deform significantly under relatively low stress. This is because that at the beginning of the loading, LGBB sample is loose, there is a lot of void between the gangue particles. When the external pressure is loaded, the gangue particles can cause frequent movement and fill the void to make the specimen undergo a large deformation. In the slope fast increase stage, the strain-stress relationship of LGBB changes exponentially. The deformation-resistant ability spirals up. This is because that the LGBB sample has been compacted after the first stage. The internal void of the sample was significantly reduced, and the particle movement

was restricted. The deformation of the sample during this stage was mainly due to the failure of the gangue block under great pressure.

In the stable linear stage, high stress generates only limited strain, i.e. the deformation-resistant ability of LGBB hives and their load bearing capability stays stable. This is because that the LGBB sample has established a stable bearing structure at this stage, the void is basically compacted, and the particles are not easily broken again. Most of the deformation produced during this stage is elastic deformation.

(2) The approximate linear stage of all three graded LGBB take place in the strain range of 0-0.2, and the stable linear stage of them in the strain range of 0.31, 0.38 and 0.35 respectively. In addition, under the same strain, #1 graded LGBB are subject to the largest amount of stress, followed by #3 and #2. Therefore, under the same compression condition, balanced-sized graded gangues reach the stable linear stage the fastest and have the best deformation-resistant ability. This is due to the better coordination between large particles and small particles in the balanced-sized graded gangues sample. When the sample is under pressure, the small particles can be quickly filled into the void of the sample, so that the sample can reach a stable bearing structure faster.

(3) When the load stress reaches 21 MPa, the biggest strain of all three graded LGBB is 0.41-0.46, whereas the strain of the large-particle-dominated graded gangues is the largest and the balanced-sized group is smallest. Therefore, using balanced-sized graded gangues, due to the collaboration between the different sized masses, the deformation-resistant ability of LGBB will be effectively boost.

### ***3.2 Features of LGBB failure during confined compression***

Taking the ending strains of the initial load bearing stage and the accelerated load bearing stage as the loading termination condition, two staged confined compression tests are performed to each of the three graded LGBB. The result of such tests are compared with the previous complete confined compression tests. In doing so, the fragmentation of test samples in each of the three stages can be analyzed. Taken #1 (balanced-sized graded gangues) for an example, loading stops when strain reaches 0.2 in the first staged test and 0.31 in the second one. The fragmentation of #1 graded LGBB in each stage is shown in Figs. 9(a-d).



(a) Before compression



(b)  $\varepsilon=0.2$



**Figure 9:** State of fragmentation in each stage after compression of #1

From Fig. 9:

In the approximate linear stage, fragmentation of the #1 graded LGGB is not obvious. In this stage, the deformation-resistant ability is rather weak. Deformation of sample gangues are mainly caused by block displacement and overturn, and the resulted pore compression. However, both gangues containing joints and relatively low strength are found to be fragmented, as shown in Fig. 9(b). Fig. 9(c) demonstrates the fragmentation state of gangues in the later part of the slope fast increase stage. Compared with the approximate linear stage, large quantity of gangues fragment as axial stress accumulates along with further compression. This is because the LGGB sample has been compacted after the first stage. The contact form between particles is mostly line-line and point-surface contact, and the particles can be broken in large amount due to stress concentration under external loading. Fig. 9(d) shows the failure of gangues in the later part of the stable linear stage. Compared with the previous stage, i.e. the slope fast increase stage, gangue particles continue to fragment, but fragmented particles account for a smaller percentage in the total test samples. Deformation of gangues in this stage mainly results from the displacement and overturn of the fragmented small-particle blocks, which fill the pores surrounding them.

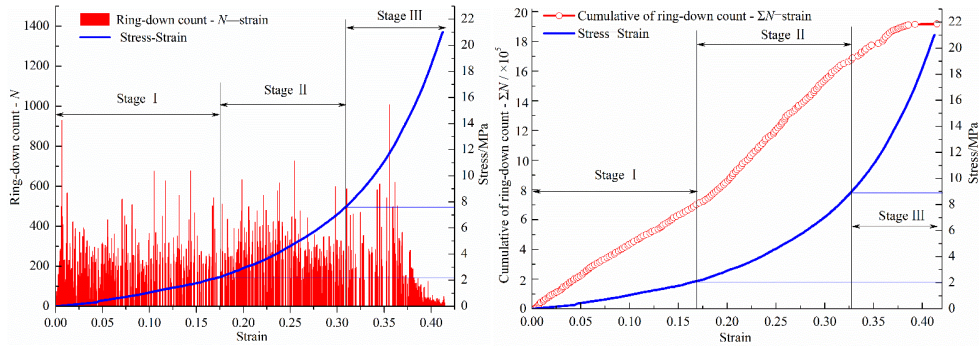
#### **4 AE features of graded LGGB during confined compression**

Coal-rock mass AE monitoring techniques are mainly employed to analyze the AE rules by observing the change of AE parameters over time-time is the basic variable in the monitoring and prediction process [Huang and Liu (2013)]. This experiment uses strain control loading regime and strain and time show linear correlation. Therefore, changing patterns of ring-down counts ( $N$ ) and cumulative of ring-down counts ( $\Sigma N$ ), as well as the spatial distribution pattern of AE events at different time points are monitored, so as to analyze the space-time evolution rules of AE of graded gangues during confined compression. For the purpose of this article, AE signal incurred by mutual restraints and collision among blocks are defined to be friction type AE, and that incurred by the fragmentation of blocks is defined to be breaking type AE.

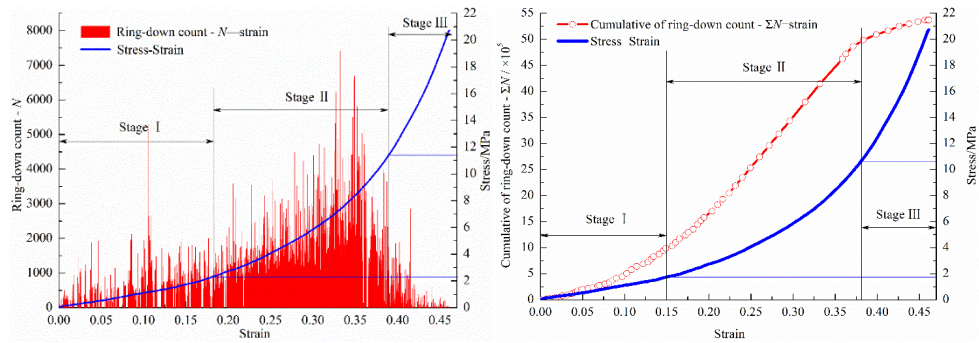
##### **4.1 AE ring-down counts-strain relationship**

The relationship between stress and strain, ring-down counts and strain, cumulative of ring-

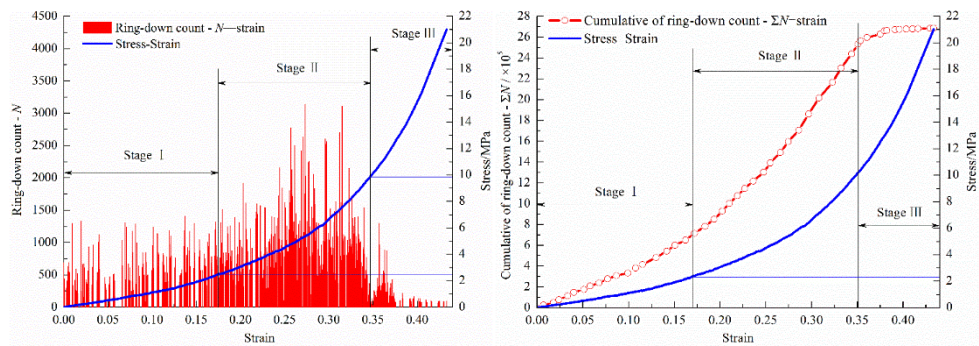
down counts and strain of different graded LGBB during confined compression are demonstrated with the curves in Figs. 10(a-f). The cumulative of ring-down counts in different compaction stages of different graded LGBB are counted as shown in Tab. 3.



(a)#1 graded gangue ring-down counts (b)#1 graded gangue cumulative of ring-down counts



(c)#2 graded gangue ring-down counts (d)#2 graded gangue cumulative of ring-down counts



(e)#3 graded gangue ring-down counts (f)#3 graded gangue cumulative of ring-down counts

**Figure 10:** Ring-down counts-strain relationship curve of graded gangue

**Table 3:** The cumulative of ring-down counts in different compaction stages

The cumulative of ring-down counts ( $\Sigma N/ \times 10^5$ )	Stage I	Stage II	Stage III	Total
#1	7.3	9.2	2.5	19.0
#2	10.0	39.5	4.0	53.5
#3	7.0	18.4	1.6	27.0

From Fig. 10 and Tab. 3:

(1) In the process of confined compression of all three graded LGBB, both ring-down counts-strain curve and cumulative of ring-down counts-strain curve are highly correlated with the strain-stress curve. The whole AE process can be divided into three periods, i.e. the developing period, the active period and declining period, corresponding to the approximate linear stage, the slope fast increase stage and the stable linear stage of the deformation process, respectively.

(2) In the developing period, as AE signals are sparse and ring-down counts remains low, slope of cumulative of ring-down counts-strain curve is small. As per the analysis by this article, this is because in the approximate linear stage, due to high porosity and the weak mutual restraints effect between gangue masses, they are liable to move and overturn to fill the surrounding pores. Therefore, the AE events in this stage are primarily friction type AE resulted from the friction and collision among particles. A few jump signals are also monitored, mainly caused by the breaking type AE incurred by the fragmentation of gangues containing joints or relative low strength.

(3) As the strains increasing, LGBB transit into the slope fast increase stage and AE events into their active period. AE signals become increasingly dense, so do the jump signals. Slope of cumulative of ring-down counts-strain curve is much steeper. This is because the LGBB sample has been compacted after the first stage. The internal void of the sample was significantly reduced, and the particle movement was restricted. In this stage the contact form between particles is mostly line-line and point-surface contact, and the particles can be broken in large amount due to stress concentration under external loading, resulting in a large number of breaking type AE. At the same time, as test samples go back to unstable structure, particles start to slide and overturn again in large scale and incur friction type AE. In this period, test samples change back and forth between stable and unstable structures, and AE signals are the co-production of friction type AE and breaking type AE.

(4) As the strains continue increasing, AE activities move into declining period and the deformation process into the stable linear stage. This is because the LGBB sample has established a stable bearing structure at this stage, the void is basically compacted, and the particles are not easily broken again. In this stage, most AE signals are incurred by friction type AE, caused by the friction and collision of blocks when they slide and overturn like they do in the developing period. Occurrence frequency of the jump signals significantly decrease and cumulative of ring-down counts-strain curve becomes flat, suggesting that the probability for secondary breakup of gangues after they fragment into smaller masses

is low, and their AE events are extremely inactive.

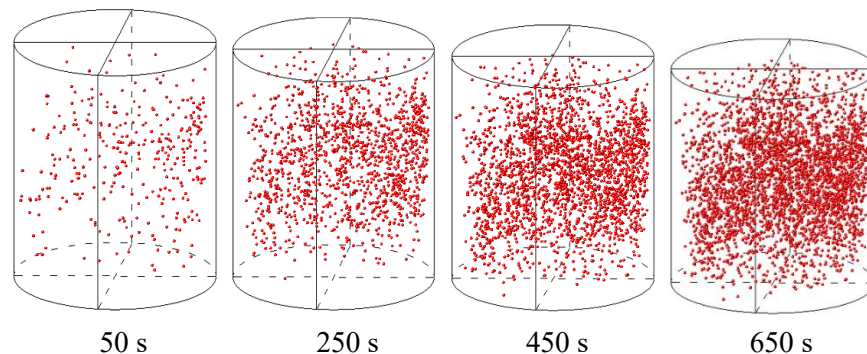
(5) The cumulative of ring-down counts of #1, #2 and #3 graded gangues in the whole compression process are  $19 \times 10^5$ ,  $53.5 \times 10^5$  and  $27 \times 10^5$ , respectively. In the active period of AE, the cumulative of ring-down counts of the three groups are  $9.2 \times 10^5$ ,  $39.5 \times 10^5$  and  $18.4 \times 10^5$ , accounting for 48.4%, 73.8% and 68.1% of their own total cumulative of ring-down counts in the whole process. As per these numbers, #2 graded gangues are the most active in terms of their AE events, followed by #3 and #1. In particular, AE events of #2 graded gangues concentrate in the active period, while those of #1 are evenly distributed at a low level through the whole process. This is because the initial void ratio of the large-particle-dominated graded gangues is high, and this allows blocks to move actively in the initial stage. Later, along with the high stress concentration, blocks fragment in quantity. In the contrast, for the small-particle-dominated graded gangues, both the initial void ratio and the strain concentration are low, causing only few gangues to fragment in the later stage. As for balanced-sized graded gangues, the collaboration between large-particle blocks and small ones, i.e. large-particle blocks form a confined skeleton while small ones fill the pores in such skeleton and assume part of the extrusion force, conspicuous weak the strain concentration among large-particle blocks and fragmentation.

#### 4.2 Spatial distribution of AE events

The previous two sections explained the time features of AE parameters along with the change of strain, but only by studying the time features cannot reflect the whole peculiarity of AE during confined compression. It is more convictive that combined time features with spatial distribution features of AE events. Therefore, this experiment also monitored the space positioning of AE events.

It is observed that the spatial distribution of AE events of graded LGBB during confined compression follows similar patterns. Due to space constraints of this article, only the test results of #1 graded gangue can be elaborated here.

Four typical time points are selected to analyze the evolution of spatial distribution. Spatial distribution of AE events of #1 graded LGBB at each of the four times points are shown in Fig. 11(a-c).



(a) 3D image of AE events spatial distribution evolution

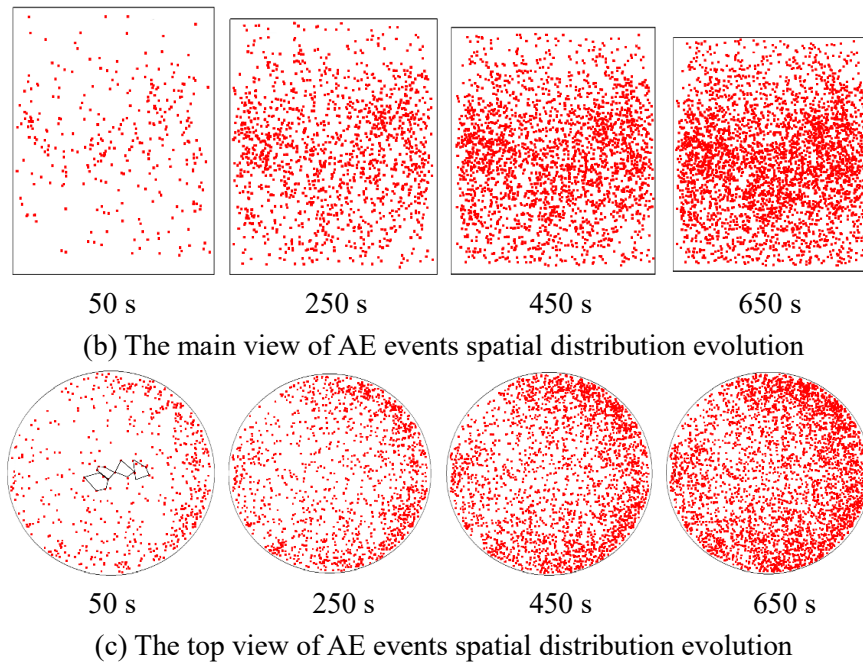


**Figure 11:** AE events spatial distribution evolution

From Fig. 11:

- (1) When the loading just begins (the first 50 s), the location points of AE events are distributed sporadically in the test samples. The reason for this phenomenon is that in the initial loading period, due to the mutual friction and collision of blocks, AE of LGBB samples are mainly friction-induced, and that there is only limited rock mass fragmentation. Therefore, AE events mainly take place in the contact points over the edges of blocks, and a blank area for AE events is formed inside of these edges.
- (2) As the loading continues, the location points of AE events start to penetrate into the blank area and become denser. The reason is that as the strain inside of the samples goes up and the extrusion force among blocks also increases, large amount of blocks fragment and correspondingly, breaking type AE massively takes place inside of blocks.
- (3) In the whole loading process, monitoring from the axial direction, the middle part of samples have much more location points of AE events than the two ends. The monitoring from the radial direction, the edges of samples have much more location points than the inside part. This indicates that in the process of confined compression, AE events are most active on the edges of the middle part of test samples. The reason is that during confined compression, LGBB tend to move sideways, and the tendency to move from the center of the steel cylinder to the edges and from the two ends to the middle become stronger over time. But such tendency is restrained by the firm cylinder extensine, gangues will fragment in quantity at the edges of the sample, especially those in the middle part.

## 5 Conclusion

This article introduces the AE systems to conventional confined compression test, AE

patterns of different graded LGBB in different stages of compression are studied in this article by monitoring the AE parameters of LGBB during confined compression. The main conclusion are as follows:

- (1) Balanced-sized graded LGBB reach the stable linear stage the fastest and have the lowest level of strain and the best deformation-resistant ability.
- (2) The AE parameters is highly correlated with the strain-stress curve. In the approximate linear stage of confined compression, AE events are in developing period and AE signals are mainly contributed by friction type AE. In the slope fast increase stage, AE events are in their active period and AE signals are the results of both friction type AE and breaking type AE. In the stable linear stage, AE events are in their declining period and AE signals are incurred mainly by friction type AE, again.
- (3) In the whole compression process, compared with the large-particle-dominated graded gangues and small-particle-dominated graded gangues, the AE ring-down counts and AE energy of balanced-sized graded gangues are more balanced at a generally lower level. AE parameters of the large-particle-dominated graded gangues are the highest across all compression stages and small-particle-dominated graded gangues rank in the middle.
- (4) In the initial loading period, there is a lot of blank area for AE events inside the test samples. As the loading continues, the location points of AE events start to spread to the blank area and become denser. In the whole loading process, monitoring from the axial direction, the middle part of samples has much more location points of AE events than the two ends. The monitoring from the radial direction, the edges of samples have much more location points than the inside portion.

**Acknowledgments:** Financial support for this work provided by the Fundamental Research Funds for the Central Universities (2017BSCXA20) and Postgraduate Research & Practice Innovation Program of Jiangsu Province (KYCX17\_1552) are gratefully acknowledged.

**Conflict of Interest:** The authors declare that there is no conflict of interest regarding the publication of this paper.

## References

- Ai, T.; Zhang, R.; Liu, J.; Zhao, X.; Ren, L.** (2012): Space-time evolution rules of acoustic emission locations under triaxial compression. *Journal of the China Coal Society*, vol. 36, no. 12, pp. 2048-2057.
- Browning, J.; Meredith, P. G.; Stuart, C. E.; Healy, D.; Harland, S. et al.** (2017): Acoustic characterization of crack damage evolution in sandstone deformed under conventional and true triaxial loading. *Journal of Geophysical Research-Solid Earth*, vol. 122, no. 6, pp. 4395-4412.
- Calvetti, F.; Combe, G.; Lanie, R. J.** (1997): Experimental micromechanical analysis of a 2D granular material: relation between structure evolution and loading path. *International Journal for Numerical & Analytical Methods in Geomechanics*, vol. 2, no. 2, pp. 121-163.
- Cao, Z.; Du, F.; Li, Z.; Wang, Q.; Xu, P. et al.** (2017): Research on instability mechanism

and type of ore pillar based on the fold catastrophe theory. *Computer Modeling in Engineering & Sciences*, vol. 113, no. 3, pp. 275-293.

**Du, K.; Li, X.; Li, D.; Weng, L.** (2015): Failure properties of rocks in true triaxial unloading compressive test. *Transactions of Nonferrous Metals Society of China*, vol. 25, no. 2, pp. 571-581.

**Fedorov, V. V.** (1974): Regression problems with controllable variables subject to error. *Biometrika*, no. 61, pp. 49-55.

**Geiger, L.** (1912): Probability method for the determination of earthquake epicenters from the arrival time only. *Bull. Saint Louis University*, no. 8, pp. 60-71.

**Huang, B.; Liu, J.** (2013): The effect of loading rate on the behavior of samples composed of coal and rock. *International Journal of Rock Mechanics and Mining Sciences*, no. 61, pp. 23-30.

**Huang, Y.** (2012): *Ground control theory and application of solid dense backfill in coal mines (Ph.D. Dissertation)*. China University of Mining and Technology, Xuzhou, China.

**Huang, Y.; Zhang, J.; Zhang, Q.; Nie, S. J.; An, B. F.** (2012): Strata movement control due to bulk factor of backfilling body in fully mechanized backfilling mining face. *Journal of Mining and Safety Engineering*, vol. 29, no. 2, pp. 162-167.

**Ingraham, M. D.; Issen, K. A.; Holcomb, D. J.** (2013): Use of acoustic emissions to investigate localization in high-porosity sandstone subjected to true triaxial stresses. *Acta Geotechnica*, vol. 8, no. 6, pp. 645-663.

**Lei, X. L.; Masuda, K.; Nishizawa, O.; Jouniaux, L.; Liu, L. et al.** (2004): Detailed analysis of acoustic emission activity during catastrophic fracture of faults in rock. *Journal of Structural Geology*, vol. 26, no. 2, pp. 247-258.

**Li, J.; Yue, J.; Yang, Y.; Zhao, L.** (2016): Acoustic emissions waveform analysis for the recognition of coal rock stability. *Journal of the Balkan Tribological Association*, vol. 22, no. 1, pp. 220-226.

**Li, M.; Zhang, J.; Zhou, N.; Zhang, Q.** (2017): Deformation and failure analysis of river levee induced by coal mining and its influence factor. *Computer Modeling in Engineering & Sciences*, vol. 113, no. 2, pp. 183-194.

**Liu, Z.** (2014): *Compaction properties of gangue and its application in backfilling coal mining (Ph.D. Dissertation)*. China University of Mining and Technology, Xuzhou, China.

**Lu, Y.; Song, C.; Jia, Y.; Xia, B.; Ge, Z. et al.** (2015): Analysis and numerical simulation of hydrofracture crack propagation in Coal-Rock bed. *Computer Modeling in Engineering & Sciences*, vol. 105, no. 1, pp. 69-86.

**Mansurov, V. A.** (1994): Acoustic emission from failing rock behavior. *Rock Mechanics and Rock Engineering*, vol. 27, no. 3, pp. 173-182.

**Mao, W.; Aoyama, S.; Goto, S.; Towhata, I.** (2015): Acoustic emission characteristics of subsoil subjected to vertical pile loading in sand. *Journal of Applied Geophysics*, vol. 119, pp. 119-127

**Masad, E.; Saadeh, S.; Al-Rousan, T.; Garboczi, E.; Little, D.** (2005): Computations of particle surface characteristics using optical and X-ray CT images. *Computational*

*Materials Science*, vol. 34, no. 4, pp. 406-424.

**Meng, Q.; Zhang, M.; Han, L.; Pu, H.; Li, H.** (2016): Effects of size and strain rate on the mechanical behaviors of rock specimens under uniaxial compression. *Arabian Journal of Geosciences*, vol. 9, no. 8.

**Miao, X.; Zhang, J.; Guo, G.** (2010): Study on waste-filling method and technology in fully-mechanized coal mining. *Journal of China Coal Society*, vol. 35, no. 1, pp. 1-6.

**Miao, X.** (2012): Progress of fully mechanized mining with solid backfilling technology. *Journal of China Coal Society*, vol. 37, no. 8, pp. 1247-1255.

**Michlmayr, G.; Or, D.** (2012): Mechanisms for acoustic emissions generation during granular shearing. *Granular Matter*, vol. 16, no. 5, pp. 627-640.

**Qin, S.; Li, Z.; Zhang, Z. et al.** (1993): *An introduction to acoustic emission technique sin rocks*. South West Jiao Tong University Press, Chengdu, China.

**Rudajev, V.; Vilhelm, J.; Lokajicek, T.** (2000): Laboratory studies of acoustic emission prior to uniaxial compressive rock failure. *International Journal of Rock Mechanics & Mining Sciences*, vol. 37, no. 4, pp. 699-704.

**Tarantola, A.; Valette, B.** (1982): Inverse problem quest for information. *J. Geophys*, vol. 2, no. 1, pp. 24-39.

**Wang, G.** (2005): *Studies on the recovery of coal gangues in Fuxin District Liaoning Province (Master Dissertation)*. Chengdu University of Technology, Chengdu, China.

**Wu, X.** (2014): *Mechanical properties of solid filling materials research and application*. Master Dissertation, China University of Mining and Technology, Xuzhou, China.

**Zhang, L.; Zhang, J.; Zhang, G.; Sun, Z.** (2008): Development and application of a 2D biaxial compression test system for granular materials. *Chinese Journal of Geotechnical Engineering*, vol. 30, no. 1, pp. 148-152.

**Zhong, X.; Yuan, J.** (1992): Dilatancy model of granular materials. *Rock Soil Mechanics*, no. 13, pp. 1-10.